ANALYSIS OF A ROTATING PLASMA EXPERIMENT

Peter M. Sockol*

Department of Mechanical Engineering,

Massachusetts Institute of Technology,

Cambridge, Massachusetts

29111

In experiments with a homopolar device Fahleson has observed that for low values of the discharge current the voltage drop across the plasma is proportional to the magnetic field and independent of the current and pressure. The rotational velocity corresponds to a kinetic energy for the ions equal to the ionization potential of the gas. These experiments have been analyzed using a steady-state continuum model of the flow in which the bulk of the gas rotates at a uniform velocity and the current is confined to thin Hartmann boundary layers on the end-walls. The voltage drop has been calculated as a function of current, pressure, magnetic field, and atomic species. The dependence on these parameters is in good agreement with the measurements under all conditions, while the magnitude of the voltage is generally smaller than the observed value by a factor of two. Author

1. INTRODUCTION

Since the homopolar experiments of Fahleson and his co-workers[1,2], there has been considerable interest in the limiting voltage observed in these rotating plasma experiments. In the homopolar device a test gas is confined in the annular space between two coaxial electrodes in an axial magnetic field. The gas is simultaneously ionized and set into rotation by the discharge of a capcitor bank across the electrode gap and the interaction between the radial current and the axial magnetic field.

In Fahleson's experiments the current was limited by a series resistor and the magnetic field was given a mirror configuration to protect the end-walls. During the discharge the voltage was relatively constant for about 60 μ sec. and the current decayed by a factor of two or three in the same period. For currents below a few kA , depending on the pressure, it was observed that the voltage was insensitive to variations in current and gas pressure, and directly proportional to the magnetic field strength. The rotational velocity, calculated from the voltage, magnetic field strength, and electrode spacing, gives a kinetic energy for the ions approximately equal to the ionization potential of the gas. Doppler shift measurements, obtained by reversing the magnetic field, were consistent with these rotational velocities. In addition the lack of variation of the velocity when the electrode radii were changed indicates that the rotational velocity was constant over most of the volume. This "ionization velocity" has been observed in H_2, D_2, He, N_2, O_2, and A in these experiments[2], the velocity being based in all cases on the atomic ion. The same limiting velocity has been observed in rectilinear plasma accelerators[3,4], while higher limiting velocities have been observed in other types of rotating plasma experiments[5,6].

Alfvén[7] has interpreted Fahleson's results in terms of a strong ionizing interaction which, it is proposed, takes place whenever a neutral gas moves through a plasma in a magnetic field at the above "ionization velocity." The first comprehensive analysis of these observations, however, was that of Lin[8]. Lin's model is that of a quasi-steady state free-molecular flow in which the logarithmic rates of change of the plasma velocity and temperature are small compared to the logarithmic rate of change of the plasma density. The instantaneous flow of energy into the plasma goes into ionization and acceleration of the gas, radiation to the walls, and loss of particles to the walls. Rotation and heating of the neutral atoms is neglected and the plasma is assumed to be spatially homogeneous. Ionization is produced by electron impact and the electrons, because of their very large Hall parameter, are in turn heated by elastic collisions with the ions rather than directly by the electric field. Lin's theory predicts a rotational velocity that is in excess of the "ionization velocity" by an amount depending on the thermal energy of the plasma and the magnitude of the radiation loss. By varying the degree of ionization at fixed current to find the minimum attainable voltage, a curve of voltage vs. current is obtained which has a form that is in good agreement with the experimental one. The level of the constant voltage varies from slightly above the observed value to more than 50% in excess of this value as the gas is varied from optically thick to optically thin to line radiation. More recently Hassan[9] has obtained a portion of Lin's results using the conservation equations for the different species and neglecting losses.

Another explanation of Fahleson's results has been proposed by Dobryshevskii[10] and extended by Lehnert[11]. Dobryshevskii considers the heating of an electron moving through a stationary neutral gas at an E/B drift velocity of the order of the "ionization velocity." He shows that most of this heating would come from the transverse electric field rather than Coulomb collisions with the ions provided that the ion thermal energy is less than the drift energy and the degree of ionization is not too large. The analyses in Refs. 10 and 11 use a steady-state continuum model in which the neutral gas is stationary and the direct heating of the electrons by the electric field is balanced by collisional losses. The electron temperature is determined through the balance between volume ionization and ambipolar diffusion along the magnetic field to the end-walls. The voltage obtained from these analyses is directly proportional to the magnetic field; however, it is also a strong function of pressure. Over most of the pressure range covered in the experiments the voltage obtained by Lehnert is well above the observed value.

In Fig. 1 the net mean free path λ^a for a neutral atom moving at the "ionization velocity" through dissociated H_2 and N_2 is given as a function of pressure p^o and degree of ionization α. The strong decrease in λ^a with increasing α is due to the large cross-section for charge exchange with the ions. In Fahleson's experiments the pressure ranged from 10 to 150 μ Hg. and a typical dimension of the annular test chamber was of the order of 10 cm. Thus fig. 1 shows that, except for the lowest values of p^o and α, λ^a was at least a factor of ten smaller than the dimensions of the device. A few simple calculations suffice to show that λ^a was larger than any of the other relevant mean free paths. It is likely, therefore, that a continuum analysis would be more appropriate to the experimental conditions than a free-molecular one. The question of whether or not there was a large slip between the atoms and the ions is a more difficult one as it concerns the transition range of flow intermediate between free-molecule and continuum flow. Nevertheless, under the near continuum conditions of the experiments it seems unlikely that there could have been substantial slip between the atoms and the ions. From this point of view there is an inconsistency in Dobryshevskii's model. It is doubtful that ambipolar diffusion of charged particles along the magnetic field is compatible with a large slip between the charged particles and the neutral atoms perpendicular to the field.

During the constant voltage portion of the discharge time, the energy fed into the gas in a typical run was substantially greater than that required to completely ionize and accelerate the gas. This suggests that the flow was largely governed by a steady-state balance between the power input and the various energy losses from the system. In section 6 it will be shown that there was insufficient time during the experiment for diffusion processes to relax to a steady-state, but that this has only a weak effect on the present results.

The effects of viscous drag at the boundaries in rotating plasma experiments has been discussed by Kunkel et. al.[12] They find that if there is contact between the plasma and the insulators, the current will tend to concentrate in thin boundary layers close to the insulators, however they do not investigate the structure of these layers. In the present work these ideas are combined with those of Dobryshevskii[10] concerning the diffusion of charged particles along the magnetic field to the end-walls. The resulting steady-state continuum theory is used to analyze the rotating plasma experiments of Fahleson and his co-workers.

2. PHYSICAL MODEL AND BASIC ASSUMPTIONS

In the present analysis the model is that of a steady-state rotating Hartmann flow[13]. The bulk of the gas including the neutral atoms rotates at a uniform velocity and the current is confined to thin boundary layers on the end-walls. The axial magnetic field B and the radial electric field E are constant throughout the volume. As the electron Hall parameter is much greater than one, the effective conductivity of the ions is much greater than that of the electrons in the radial direction and most of the radial current is carried by the ions. In the absence of a large slip between the electrons and the atoms, most of the electron heating should be due to Coulomb collisions with the ions, although this is not assumed a priori. In order to accomplish this heating the heavy particle temperature rises somewhat above the electron temperature in the core flow. The electrons are thermally insulated from the end-wall by a sheath; thus most of the energy received by the electrons goes into ionizing collisions with the atoms.

As continuum equations are used to describe the flow, it is assumed that all mean free paths are small compared to the thickness of the Hartmann layer. The transport properties are taken to be constant and are evaluated using appropriate average values for the electron density and the temperature. Since the thermal conductivity of the electrons is much greater than that of the heavier particles, the electron temperature T^e is taken as constant. The effects of centrifugal and coriolis forces are neglected as are all variations in directions perpendicular to the magnetic field.

Conditions under which this is permissible are developed in Ref. 14. The sheaths on the electrode surfaces are also ignored and quasi charge neutrality is assumed to hold throughout the volume. In the case of diatomic gases, such as H_2 and N_2, it is assumed that they are completely dissociated under the operating conditions of the experiments. Since a proper treatment of line radiation is quite difficult, all effects of radiation are neglected. The net ionization rate is taken as the difference between electron-atom ionization and three-body recombination. The effect of collisional transitions between excited states is included in the rate coefficients.

3. SIMPLIFIED ANALYSIS

According to the physical model of the flow, the rate at which energy is lost from the system is dependent on the structure of the boundary layers on the end-walls. Profiles of velocity, gas temperature, and electron number density corresponding to the model are sketched in Fig. 2. The core velocity v_c is set equal to E/B as there is no current in the core. In this section elementary arguments based on these profiles are used to develop a simplified explanation of the experimental observations.

In the Hartmann boundary layer the wall shear stress is balanced by the integrated magnetic force,

$$\mu v_c / \delta_m \approx \sigma_\perp E B \, \delta_m ,$$

or

$$\delta_m^{-1} \approx B (\sigma_\perp / \mu)^{1/2} \tag{3.1}$$

where μ is the viscosity and $\sigma_\perp$ the effective electrical conductivity in a direction perpendicular to the magnetic field.

The thermal boundary layer thickness δ_t is determined by the behaviour of the viscous and ohmic heating of the gas. The velocity gradient and the current decay from a maximum at the wall in the Hartmann thickness δ_m. Since the viscous and ohmic heating are proportional to the square of these two quantities respectively, the heating effects decay in half the Hartmann thickness, $\delta_t \approx 1/2\delta_m$. The total energy input to the flow is equal to the integrated viscous and ohmic heating. This is in turn balanced by the heat conducted to the wall and the ionization energy carried to the wall by the diffusing electron-ion pairs,

$$[\,\mu(v_c/\delta_m)^2 + \sigma_\perp E^2]\delta_t \approx \kappa^h T^a/\delta_t + \varepsilon_i D_a n_c^e/\delta_a,$$

or
$$1/2\ (E/B)^2 \approx (\kappa^h/\mu)T^a + (\varepsilon_i D_a n_c^{\,e}/\mu)\ \delta_t/\delta_a, \tag{3.2}$$

where κ^h is the thermal conductivity of the heavy particles, ε_i the ionization potential, and D_a the ambipolar diffusion coefficient.

As indicated by the temperature profile (Fig. 2b), a small amount of heat is conducted toward the core. This is balanced by the integrated energy transfer to the electrons,

$$\kappa^h(T^a - T^e)/\delta_e \approx 3(m^e/m^a)\ \nu^e n_c^e\ k(T^a - T^e)\delta_e,$$

or
$$\delta_e^{-1} \approx [3(m^e/m^a)\nu^e\ n_c^e\ k/\kappa^h]^{1/2}, \tag{3.3}$$

where ν^e is the total collision frequency for electrons with ions and atoms, m^e/m^a is the electron-atom mass ratio, and k is Boltzmann's constant. The electron heating is balanced by volume ionization and the subsequent diffusion of electron-ion pairs to the wall,

$$\kappa^h(T^a - T^e)/\delta_e \approx \varepsilon_i D_a n_c^e/\delta_a,$$

or
$$T^a \approx T^e + (\varepsilon_i D_a n_c^e/\kappa^h)\delta_e/\delta_a. \tag{3.4}$$

Combining Eqs. (3.2) and (3.4) gives

$$1/2(E/B)^2 \approx (\kappa^h/\mu)T^e + (\varepsilon_i D_a n_c^e/\mu)(\delta_e + \delta_t)/\delta_a. \qquad (3.5)$$

This equation will be used to show the dependence of E/B on the degree of ionization α , and hence on the current through the electrical conductivity $\sigma_\perp$.

In the diffusion boundary layer (Fig. 2c) the ambipolar diffusion of electron-ion pairs to the wall is balanced by the integrated volume ionization,

$$D_a\, n_c^e/\delta_a \approx \nu_i\, n_c^e \delta_a,$$

or

$$\delta_a^{-1} \approx (\nu_i/D_a)^{1/2}, \qquad (3.6)$$

where ν_i is the ionization frequency per electron in the diffusion boundary layer. Volume recombination is assumed to be negligible near the wall where the electron density is small.

For low values of α, the diffusion thickness δ_a is limited by the end-wall half-spacing d, and volume recombination is negligible everywhere. The quantity ν_i/D_a is a function of the electron temperature T^e and the initial pressure p^o, but not of α . Thus, the relation $\delta_a \approx d$ determines T^e independent of α. In Eq. (3.5) κ^h/μ is independent of α and the second term on the right is small for low α. Therfore, E/B is independent of α. The current, however, is an increasing function of α through $\sigma_\perp$. Hence, at low α, E/B is independent of current in agreement with the experimental observations.

At higher values of α, ionization and recombination are in equilibrium in the core. This determines T^e as an increasing function of α through the Saha equation. Since ν_i increases exponentially with T^e,

δ_a becomes very small as α increases. Thus in Eq. (3.5) the second term rapidly overtakes the first, and E/B exhibits a strong increase with current, again in agreement with the observations.

4, GENERAL FORMULATION

Since the centrifugal and coriolis forces are neglected, the annular space can be replaced by an infinite straight channel with a rectangular cross-section. Cartesian co-ordinates are introduced with the main flow in the x direction, the electric field E in the y direction and the magnetic field B in the z direction. Finally, it is assumed that all variations are in the z direction.

The governing equations, in the form used here are taken from Ref. 15. They have been modified in Ref. 14 to include the effects of a magnetic field and volume ionization. With neither pressure gradient nor flow in the z direction, these equations are:

Momentum
$$\frac{d}{dz}\left(\mu\,\frac{dv_x}{dz}\right) + J_y B = 0\,, \tag{4.1}$$

$$\frac{d}{dz}\left(\mu\,\frac{dv_y}{dz}\right) - J_x B - P_y = 0\,, \tag{4.2}$$

Energy
$$(dQ/dz) = \mu(d\underset{\sim}{V}/dz)^2 + \underset{\sim}{E}^* \cdot \underset{\sim}{J} - \varepsilon_i S\,, \tag{4.3}$$

Electron Continuity
$$(d\Gamma_z^e/dz) = S\,, \tag{4.4}$$

Electron Energy
$$(dQ^e/dz) = -e\underset{\sim}{E}^* \cdot \underset{\sim}{\Gamma}^e - \varepsilon_i S + 3(m^e/m^a)\,\nu^e n^e k(T^a - T^e)\,. \tag{4.5}$$

Here Q is the total heat flux, $Q = Q^h + Q^e$, $Q^h = -\kappa^h(dT^a/dz)$,

$Q^e = -\chi^e(dT^e/dz) + \frac{5}{2}kT^e\Gamma_z^e$, and Γ_z^e the electron current density along the magnetic field. The pressure gradient P_y balances the cross flow due to the Hall effect so that there is no net mass flow in the y direction:

$$\int_{-d}^{d} \rho v_y \, dz = 0. \tag{4.6}$$

The effective electric field $\underset{\sim}{E}^*$ and the current $\underset{\sim}{J}$ perpendicular to the magnetic field are given by

$$\underset{\sim}{E}^* = \underset{\sim}{E} + \underset{\sim}{v} \times \underset{\sim}{B}, \tag{4.7}$$

$$\underset{\sim}{J} = \sigma_1 \underset{\sim}{E}^* + \sigma_2 \hat{B} \times \underset{\sim}{E}^*, \tag{4.8}$$

$$e\underset{\sim}{\Gamma}^e = -(\sigma_1 - \Omega^i\sigma_2)\underset{\sim}{E}^* - (\sigma_2 + \Omega^i\sigma_1)\hat{B} \times \underset{\sim}{E}^* \tag{4.9}$$

where $\sigma_1 = \dfrac{\sigma(1+\Omega^e\Omega^i)}{(1+\Omega^e\Omega^i)^2 + (\Omega^e)^2}$, $\sigma_2 = \dfrac{\sigma\Omega^e}{(1+\Omega^e\Omega^i)^2 + (\Omega^e)^2}$,

Ω^e and Ω^i are the electron and ion Hall parameters, and σ is the electron conductivity in the absence of a magnetic field. This form of Ohm's law includes both the Hall effect and ion slip. Along the magnetic field the diffusion current and ambipolar field are given by

$$\Gamma_z^e = \Gamma_z^i = -D_a n^e [d\,\ln(p^e + p^i)/dz], \tag{4.10}$$

$$eE_z = -kT^e(d\,\ln p^e/dz). \tag{4.11}$$

The ionization source term S is taken as the difference between an ionization rate $\nu_i n^e \equiv k_i n^e n^a$ and a recombination rate $k_r\,(n^e)^3$. The three-body recombination coefficient of Makin and Keck [16] is used for k_r. The ionization coefficient k_i is related to k_r through the principle of detailed balancing. Thus, $k_i = k_r K_e$ where K_e is the Saha equilibrium constant[17] evaluated at the electron temperature, and the source term S is written as

$$S = k_r n^e [K_e n^a - (n^e)^2]. \tag{4.12}$$

The boundary conditions on Eqs. (4.1) to (4.5) are taken as

$$z = \pm d; \quad V_x = V_y = 0, \quad T^a = T_w \approx 0, \quad (dT^e/dz) \approx 0, \quad n^e \approx 0. \tag{4.13}$$

In the diffusion controlled sheath it is assumed that most of the energy conducted into the sheath by electrons goes into ionizing collisions and acceleration of the ions toward the wall. Therefore, the electron temperature gradient approaches zero at the wall. The last condition is the common diffusion approximation, valid for small mean free paths, that the electron density approaches zero at an absorbing wall.

At constant volume the pressure p is related to the initial pressure p^o by

$$2 n^o d = \int_{-d}^{d} (n^a + n^e) dz = \int_{-d}^{d} dz\,(p - p^e)/kT^a, \tag{4.14}$$

where $n^o = p^o/kT^o$.

In addition it is convenient to introduce the current per unit length of channel I

$$I = \int_{-d}^{d} J_y\, dz\ . \tag{4.15}$$

The formulation of the problem is completed by the introduction of dimensionless variables with d, n^o, ε_i, m^a as basic parameters:

$$\bar{z} = z/d\ , \quad \bar{n} = n/n^o\ , \quad \bar{T} = kT/\varepsilon_i\ , \quad \bar{p} = p/n^o\varepsilon_i\ ,$$

$$\bar{\rho} = \rho/m^a n^o, \quad \bar{\underset{\sim}{V}} = \underset{\sim}{V}/U_i\ , \quad \bar{\underset{\sim}{J}} = \underset{\sim}{J}/e n^o U_i\ , \quad \bar{Q} = Q/n^o\varepsilon_i U_i\ ,$$

$$\bar{\underset{\sim}{E}} = \underset{\sim}{E}\, e\, d/\varepsilon_i\ , \quad \bar{\underset{\sim}{B}} = \underset{\sim}{B}\, e\, d\, U_i/\varepsilon_i\ ;$$

U_i is the "ionization velocity", $(2\varepsilon_i/m^a)^{1/2}$. The transport properties are made dimensionless by means of the same basic parameters. The only change in Eqs. (4.1) to (4.15) is that the dimensional constants are absorbed. Hence, these equations need not be reproduced, and without loss of clarity the bars will be dropped and all variables will be understood to be dimensionless.

5. CONSTANT TRANSPORT PROPERTY SOLUTION

The problem as formulated in the preceding section is still quite formidable. If the transport properties are taken as constant, however, it is possible to reduce the problem to quadratures. The resulting algebraic equations can be readily solved numerically. The superscript e on the electron density is dropped, $n^e \equiv n$.

A. Diffusion Equation

Assume $T^a \approx T^e$ =constant. Then the total density n^t is a constant and Eq. (4.14), with n an even function of z, gives

$$n^a = n^t - 2n \;, \quad n^t = 1 + \int_0^1 n \, dz \,. \tag{5.1}$$

Combining Eqs. (4.4), (4.10), (4.12), (5.1) and introducing the appropriate boundary conditions from (4.13) gives the diffusion equation for n

$$\begin{gathered} n'' + \lambda n(n^t - 2n) - \beta n^3 = 0 \,, \\ n'(0) = n(1) = 0 \,, \end{gathered} \tag{5.2}$$

with $\beta = k_r/D^a$ and $\lambda = \beta K_e$. The parameters λ and β are functions of T^e. Instead of T^e, the central degree of ionization $n_o \equiv n(0)$ is specified. The solution of (5.2) then determines T^e as a function of n_o.

The two limiting types of dependence on n_o can be obtained directly from (5.2). As $n_o \to 0$, the equation reduces to the homogeneous form $n'' + \lambda n = 0$ and $\lambda = \pi^2/4$. In this limit T^e is independent of n_o. At larger values of n_o, a different type of dependence is obtained. A necessary condition for the existence of a solution to Eq. (5.2) is $K_e\,(n^t - 2n_o) - n_o^2 > 0$. The inequality together with the definition of K_e determines a lower bound for T^e that increases without limit as $n_o \to 1$.

The solution to Eq. (5.2) is

$$z = 1 - \int_0^n dt \left\{ \lambda \left[n^t (n_o^2 - t^2) - \tfrac{4}{3}(n_o^3 - t^3) \right] - \tfrac{1}{2}\beta (n_o^4 - t^4) \right\}^{-1/2} \tag{5.3}$$

The condition $n(0) = n_o$ in (5.3), together with the definition of n^t, determines T^e as a function of n_o.

B. Momentum Equations

Equations (4.1) and (4.2) with (4.7) and (4.8) give

$$\begin{aligned} &\mu v_x'' - B^2(\sigma_1 v_x - \sigma_2 v_y) + \sigma_1 E B = 0, \\ &\mu v_y'' - B^2(\sigma_2 v_x + \sigma_1 v_y) + \sigma_2 E B - P_y = 0. \end{aligned} \tag{5.4}$$

The solution of these equations with v_x and v_y even functions of z is

$$\begin{aligned} v_x &= v_b\left[C_1 \cosh(Mz)\cos(Nz) + C_2 \sinh(Mz)\sin(Nz) + 1 - C_3\right] \\ v_y &= v_b\left[C_1 \sinh(Mz)\sin(Nz) - C_2 \cosh(Mz)\cos(Nz) - C_4\right] \end{aligned} \tag{5.5}$$

with

$$M = B(a+b)^{1/2}, \quad N = B(a-b)^{1/2}, \quad a = (\sigma_1^2 + \sigma_2^2)^{1/2}(2\mu)^{-1},$$

$$b = \sigma_1 (2\mu)^{-1}, \quad v_b = E/B, \quad \text{and} \quad \sigma_1 C_3 = \sigma_2 C_4 .$$

The boundary conditions $v_x(1) = v_y(1) = 0$, Eq. (4.6) with ρ taken to be constant, and the condition $\sigma_1 C_3 = \sigma_2 C_4$ determine the four C's.

For $\cosh M \gg 1$ the solution (5.5) has a boundary layer behaviour. The thickness of the layer is of order M^{-1}; hence M can be considered an effective Hartmann number. As the transport effects are only important within the boundary layer, the transport properties will be evaluated using the average value of the electron density across the boundary layer.

C. Heavy Particle Energy Equation

Subtracting Eq. (4.5) from (4.3) gives the heavy particle energy equation

$$\kappa^h (T^a)'' + \mu (\underset{\sim}{v}')^2 + \underset{\sim}{E}^* \cdot (\underset{\sim}{J} + \underset{\sim}{\Gamma}^e)$$
$$- 3 (m^e/m^a) \nu^e n (T^a - T^e) = 0 . \tag{5.6}$$

Introduce $\theta = T^a - T^e$. Eq. (5.6) and the associated boundary conditions (4.13), for θ even in z, are written

$$\theta'' - L^2 \theta = - (E^2/\kappa^h) h(z) ,$$
$$\theta'(0) = 0 , \quad \theta(1) \approx - T^e , \tag{5.7}$$

with

$$L^2 = 3 (m^e/m^a)(\nu^e n/\kappa^h) ,$$

$$h(z) = E^{-2} [\mu (\underset{\sim}{v}')^2 + \underset{\sim}{E}^* \cdot (\underset{\sim}{J} + \underset{\sim}{\Gamma}^e)] . \tag{5.8}$$

h(z) is independent of E.

In general $L^2\theta$ is comparable to $(E^2/\kappa^h)h$ only outside the boundary layer where h(z) is relatively small. Inside the boundary layer $L^2\theta \ll (E^2/\kappa^h)h$ and the dependence of L^2 on z is unimportant. Hence L is taken to be constant and equal to its average value L_a outside the boundary layer.

The solution to Eq. (5.7) can now be written as

$$\theta = - T^e f(z) + (E^2/\kappa^h) H(z) , \tag{5.9}$$

with
$$f(z) = \cosh(L_a z)/\cosh L_a ,$$
$$H(z) = L_a^{-1} \int_0^1 g(z,x)\, h(x)\, dx,$$
$$g(z,x) = \begin{cases} f(x) \sinh[L_a(1-z)], & \text{for } x < z; \\ f(z) \sinh[L_a(1-x)], & \text{for } x > z. \end{cases}$$

D. Electron Energy Equation

Since the electron temperature is determined by the solution of the diffusion equation, the electron energy equation can be used to obtain an expression for the electric field E. Integration of Eq. (4.5) with (4.4) from 0 to 1 and application of the boundary conditions (4.13) gives

$$(1 + \tfrac{5}{2} T^e)\, \Gamma_z^{\,e}(1) = -\int_0^1 \underset{\sim}{E}^* \cdot \underset{\sim}{\Gamma}^e dz + \kappa^h \int_0^1 L^2 \theta\, dz . \tag{5.10}$$

From Eqs. (4.7), (4.9) to (4.11)

$$-\int_0^1 \underset{\sim}{E}^* \cdot \underset{\sim}{\Gamma}^e dz = E^2 \int_0^1 F(z)\, dz - T^e D_a n_o \int_0^1 G(z)\, dz , \tag{5.11}$$

with $F(z) = E^{-2}(\sigma_1 - \Omega^i \sigma_2)\ [(E_x^*)^2 + (E_y^*)^2]$ and $G(z) = (n')^2\ (n_o n)^{-1}$. F and G are independent of E. The second integral in Eq. (5.11) diverges at its upper limit as $n(1) = 0$. The integration is cut off at a point z_s, near 1, where Γ_z^e has reached its final value and the electron drift velocity equals its random velocity. In dimensionless form

$$\Gamma_z^{\,e}(1)/n(z_s) = (m^a/m^e)^{1/2} (T^e)^{1/2} . \tag{5.12}$$

Finally, Eq. (5.10) with (5.9) and (5.11) gives

$$E^2 \int_0^1 [L^2 H(z) + F(z)]\, dz = \kappa^h T^e \int_0^1 L^2 f(z)\, dz$$
$$+ (1 + \tfrac{5}{2} T^e)\, \Gamma_z^{\,e}(1) + T^e D_a n_o \int_0^{z_s} G(z)\, dz . \tag{5.13}$$

The diffusion current to the wall $\Gamma_z^e(1)$ is of course known from the solution to Eq. (5.2).

Once E has been determined from Eq. (5.13), the current per unit length of channel I can be evaluated from Eqs. (4.15), (4.8), (4.7), and (5.5).

6. DISCUSSION OF NUMERICAL RESULTS

The numerical calculations proceed in a straightforward manner from the equations of the previous section. For fixed values of initial pressure p^o, half-spacing d, and magnetic field B, one chooses a value for the central degree of ionization n_o and solves iteratively for the electron temperature T^e. Next the transport properties are evaluated using average values for the electron density n and the gas temperature T^a. The simple approximations

$$\langle n \rangle \approx M/2 \int_{1-2/M}^{1} n \, dz \qquad \text{and} \qquad \langle T^a \rangle \approx \tfrac{2}{3} T^e$$

were used in this evaluation. Finally, the electric field E and the current per unit length I are obtained from Eqs. (5.13) and (4.15). By varying n_o an entire voltage vs. current curve can be calculated.

Such a curve of about twenty points, together with profiles of n, v_x, v_y, and T^a for each value of n_o, required about half a minute of computation time on an IBM 7090 computer.

In Fig. 3 the dimensionless velocity $\overline{E}/\overline{B}$ is plotted vs. dimensionless current per unit length $\overline{I}$ for three different gases and for conditions corresponding to the experiments. In each curve there is a relatively constant velocity section at low current followed by a rapidly increasing portion at higher currents. Since $\overline{E}/\overline{B}$ is in units of the "ionization velocity", $(2\epsilon_i/m^a)^{1/2}$, the minimum values in these curves are generally smaller than this velocity by a factor of about two. As there is considerable variation in physical properties between H_2, N_2 and Xe the close resemblance of the three curves is quite remarkable. It should be noted that diatomic gases are assumed to be completely dissociated so that an initial pressure of 30μHg. for H_2 or N_2 corresponds to a pressure of 60μHg. for the monatomic gas. All of the main features of these curves are predicted by the simplified theory of section 3.

The theory is compared with the experimental results[1,2] in Figs. 4 to 6. In these experiments the magnetic field decreased from a value B_o at the inner electrode, radius 3.5 cm., to 1/2 B_o at the outer electrode, radius 19.5 cm. In the corresponding calculations, average values of 3/4 B_o and 11.5 cm. were used for the magnetic field B and the average radius respectively. The latter quantity is needed to obtain the total current from the current per unit length of channel I.

Apart from the factor of two discrepancy in the minimum voltage, the agreement between theory and experiment in Fig. 4 is fairly good. The level portion of the curve is consistent with the data, and although the steep portion of the curve rises too rapidly the transition between the two segments occurs at about the right current. In Fig. 5 the weak logarithmic dependence of the minimum voltage on the initial pressure p^o agrees rather well with the experiment. In particular the slope of this curve is in better agreement with the data than that reported in Ref. 11. The linear dependence of the minimum voltage on the magnetic field B_o (Fig. 6) is not remarkable and has been found in previous analyses[8-11].

At low currents the diffusion processes will relax to a steady state in a time d^2/D_a. In Fahleson's experiments this time was a factor of ten greater than the experimental time of 50 to 100 μ sec. This relaxation time can be considered as the time it takes for the diffusion layers at the end-walls to grow until they meet at the center of the plasma. For shorter times the plasma should behave much like a thinner slab of plasma in a steady state. In Fig. 7 the minimum voltage is plotted vs. the end-wall half-spacing d. It is seen that a decrease in d by a factor of ten, which would make the steady-state theory formally applicable, produces little change in the results. Thus in this respect the present theory should be valid for the experimental conditions.

The numerical results reported here are not strictly applicable to the actual experimental geometry[1,2]. In Ref. 14 it is shown that the centrifugal and coriolis forces are negligible if the magnetic interaction length $\rho v_c/\sigma_\perp B^2$ is small compared to the radius r. These lengths, however, are of the same order of magnitude for most of the experimental range. The correction to the voltage drop due to the presence of electrode boundary layers is also developed in Ref. 14 for large values of the Hartmann number M. Since M is generally about 10 at the voltage minimum, this correction, which varies as $d\ell^{-1}M^{-1/2}$ where ℓ is the electrode half-spacing, is not negligible, being about a 30% correction.

The collision cross-sections used in these calculations, together with their sources, are given in Ref. 14.

7. CONCLUSIONS

The present theory can be considered successful to the extent that it predicts the general form of the experimental observations over a wide range of conditions. The shape of the voltage vs. current curve and the weak logarithmic dependence of the minimum voltage on the initial pressure are reproduced particularly well. In addition the lack of variation in the results has been demonstrated for three widely dissimilar gases. The basic ingredients of the theory are the energy balance in a Hartmann boundary layer and the relation between the electron temperature and the degree of ionization in a gas discharge. These two elements are connected by the energy exchange between heavy particles and electrons due to elastic collisions.

The most important failure of the theory is the factor of two discrepancy in the voltage. A number of factors might account for a portion of this difference. The magnetic field in Fahleson's experiments was nonuniform. It decreased by a factor of two from the inner to the outer radius and it had a 1.2 to 1 mirror ratio along the axis. This nonuniformity was not considered in the theory. The centrifugal and coriolis forces, which were not accounted for in the theory, turned out to be non-negligible. Finally, there are the effects of radiation. Lin[8] included the loss of energy by radiation in his analysis. He found that varying the fraction of the line radiation that was allowed to escape did not change the shape of the voltage vs. current curve, but that the voltage was more than 50% higher in the optically thin case than in the optically thick case. In addition the radiation can change the population of the excited states in the neutral atom which will in turn change the ionization and recombination coefficients. In any case if consideration of one or more of these mechanisms were to bring the present theory into better agreement with the experimental observations, then the "ionization velocity" would have to be regarded as a coincidence rather than a manifestation of some basic physical process.

ACKNOWLEDGMENTS

The author wishes to thank Professor J. A. Fay for suggesting both the problem and the physical model, and Professors J. C. Keck, J. L. Kerrebrock, and M. D. Cowley for many helpful discussions.

This work was supported by the National Aeronautics and Space Administration under contract NGR - 22-009-052, S/1. The work was done in part at the Computation Center at M.I.T.

FOOT NOTES

* Present address: National Aeronautics and Space Administration, Lewis Research Center, Cleveland, Ohio.

1. U. V. Fahleson, Phys. Fluids 4, 123 (1961).

2. B. Angerth, L. Block, U. Fahleson, and K. Soop, Nucl. Fusion Suppl. Pt. 1, 39 (1962).

3. J. M. Wilson, E. Pugh, A. Dattner, and J. Eninger, Phys, Fluids 7, S51 (1964) Suppl.

4. R. M. Patrick and E. R. Pugh, Phys. Fluids 8, 636 (1965).

5. D. A. Baker and J. E. Hammel, Phys. Fluids 4, 1549 (1961).

6. B. Lehnert, J. Bergström, and S. Holmberg, Nucl. Fusion 6, 231 (1966).

7. H. Alfvén, Revs. Modern Phys. 32, 710 (1960).

8. S. C. Lin, Phys. Fluids 4, 1277 (1961).

9. H. A. Hassan, Phys. Fluids 9, 2077 (1966).

10. E. M. Dobryshevskii, Zh. Tech. Fiz. 33, 1210 (1963) [English transl.: Soviet Phys. - Tech. Phys. 8, 903 (1964)].

11. B. Lehnert, Phys. Fluids 9, 774 (1966).

12. W. B. Kunkel, W. R. Baker, A. Bratenahl, and K. Halbach, Phys. Fluids 6, 699 (1963).

13. J. A. Shercliff, A Textbook of Magnetohydrodynamics (Pergamon Press, Oxford, 1965) 1st ed., p. 143.

14. P. M. Sockol, Sc. D. thesis, Massachusetts Institute of Technology (1967).

15. P. M. Sockol, NASA Technical Note D-2279 (1964).

16. B. Makin and J. C. Keck, Phys. Rev. Letters 11, 281 (1963).

17. W. G. Vincenti and C. H. Kruger, Jr., Introduction to Physical Gas Dynamics (John Wiley & Sons, Inc., New York, 1965), p. 165.

CAPTIONS FOR FIGURES

Fig. 1 Initial pressure times mean free path vs. degree of ionization for atoms in dissociated H_2 and N_2, a-i and a-a relative velocities equal "ionization velocity".

Fig. 2 Profiles corresponding to physical model: (a) velocity, (b) gas temperature, (c) electron number density.

Fig. 3 Dimensionless velocity vs. current in H_2, N_2, and Xe for B = 4500 G., d = 9 cm.

Fig. 4 Voltage vs. current in H_2 and N_2 for p^o = 30 μ Hg., B_o = 6000 G., d = 9 cm. Theory —; experiment +, o.

Fig. 5 Minimum voltage vs. initial pressure in H_2 for B_o = 5000 G., d = 9 cm. Theory -•-, experiment o.

Fig. 6 Minimum voltage vs. magnetic field in H_2 for d = 9 cm. Theory -•-, p^o = 50 μHg.; experiment x, p^o = 10 - 150 μHg.

Fig. 7 Minimum voltage vs. end-wall half-spacing in H_2 for p^o = 50 μHg., B_o = 5000 G. Theory -•-.

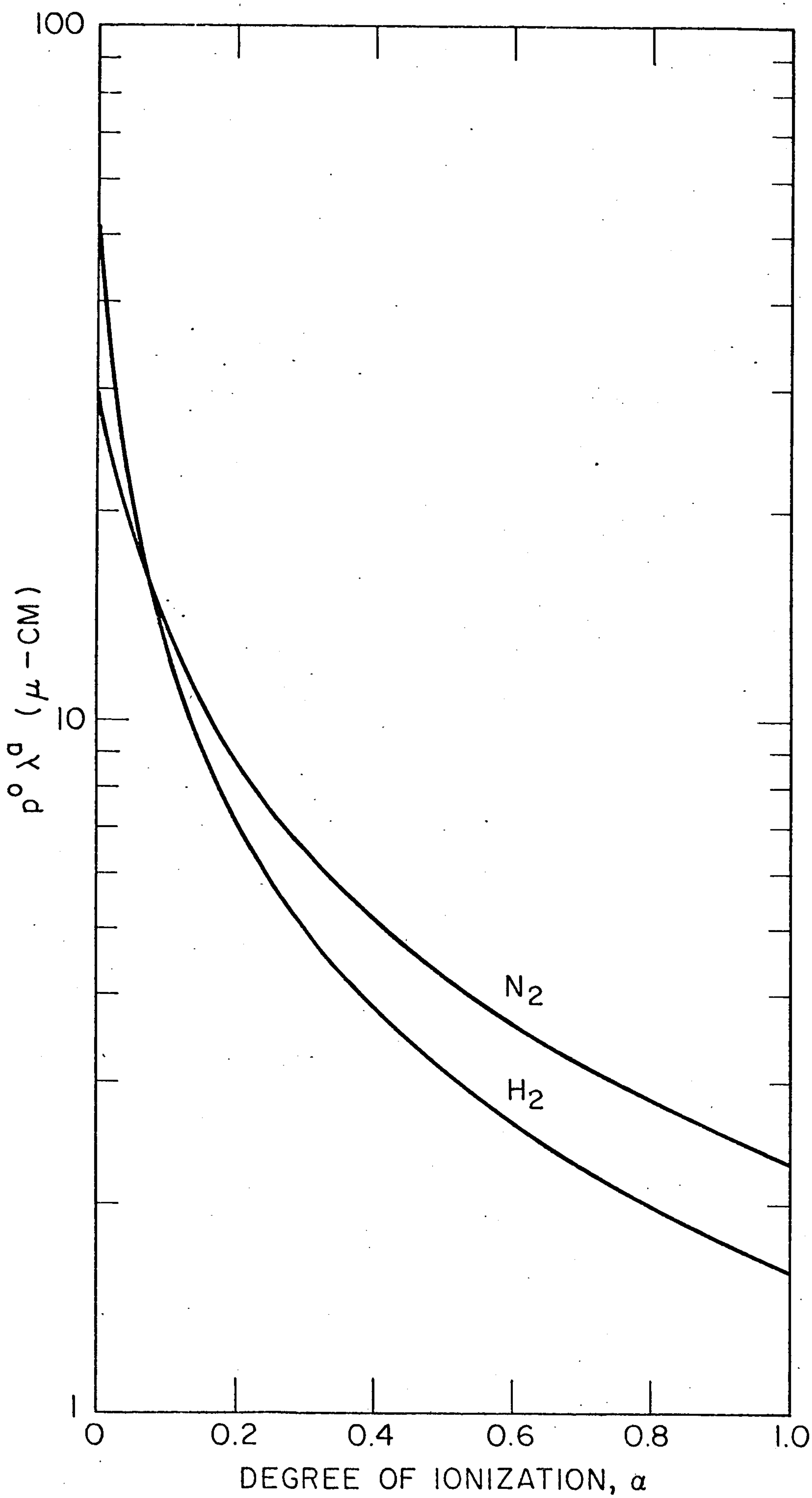

100
10
1
0
0.2
0.4
0.6
0.8
1.0
$\rho_o \lambda_a$ (μ-CM)
DEGREE OF IONIZATION, α
N_2
H_2

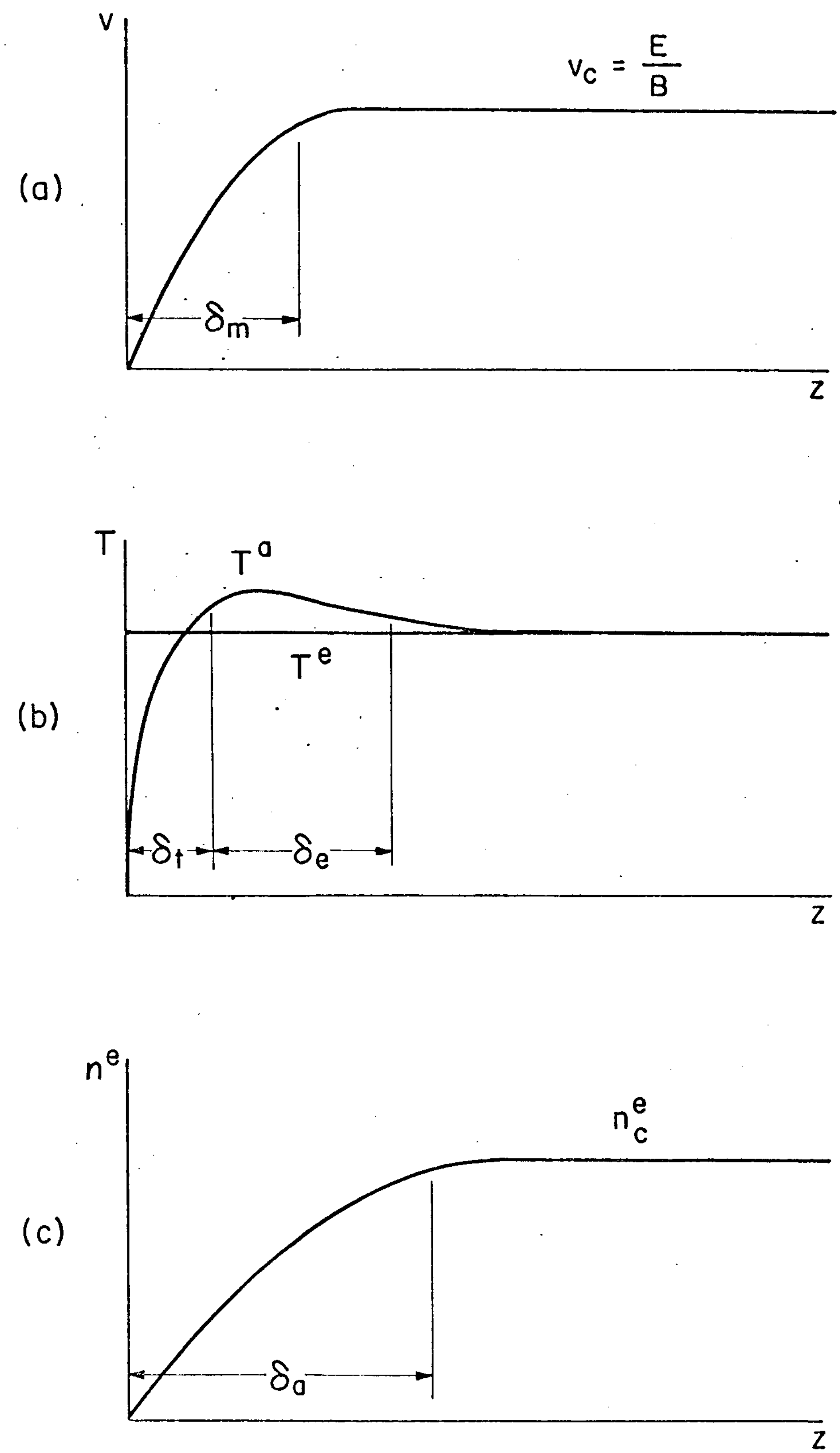

(a)
v
$v_c = \frac{E}{B}$
δ_m
z
(b)
T
T^a
T^e
δ_t
δ_e
z
(c)
n^e
n_c^e
δ_a
z

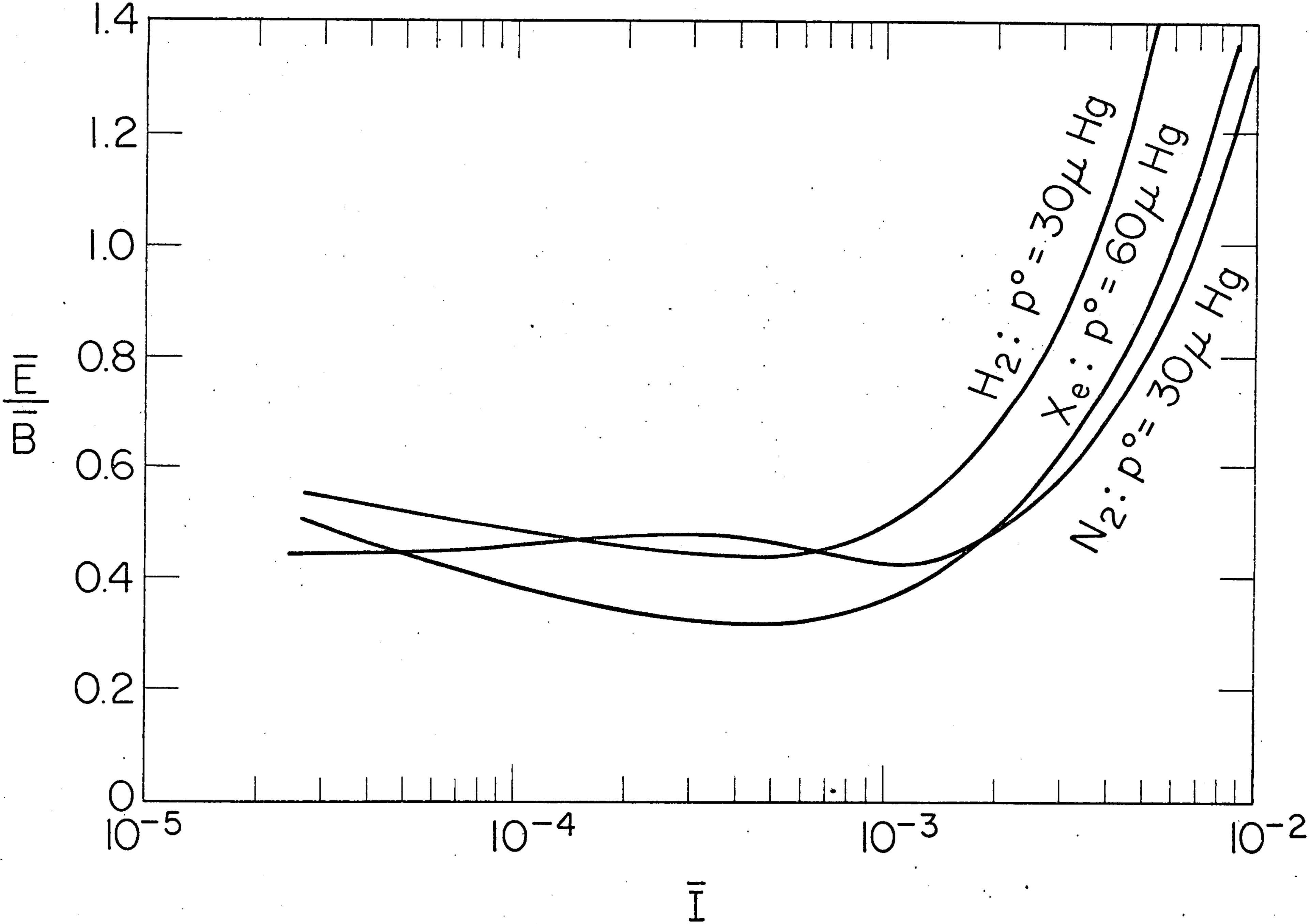

1.4
1.2
1.0
0.8
0.6
0.4
0.2
0
$\bar{E}/\bar{B}$
10^{-5}
10^{-4}
10^{-3}
10^{-2}
$\bar{I}$
H_2: p° = 30μ Hg
X_e: p° = 60μ Hg
N_2: p° = 30μ Hg

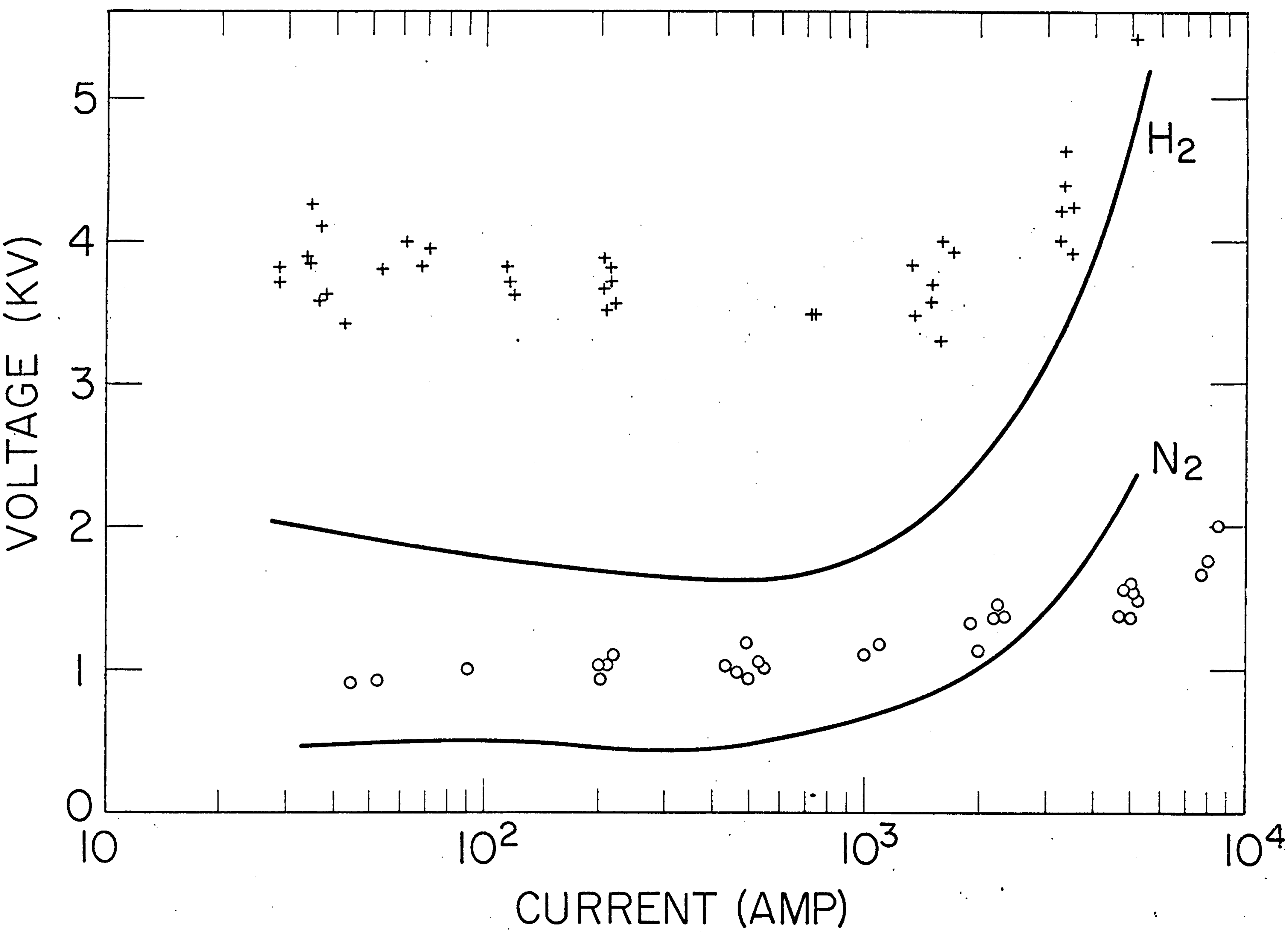

VOLTAGE (KV)
0
1
2
3
4
5
H_2
N_2
10
10^2
10^3
10^4
CURRENT (AMP)

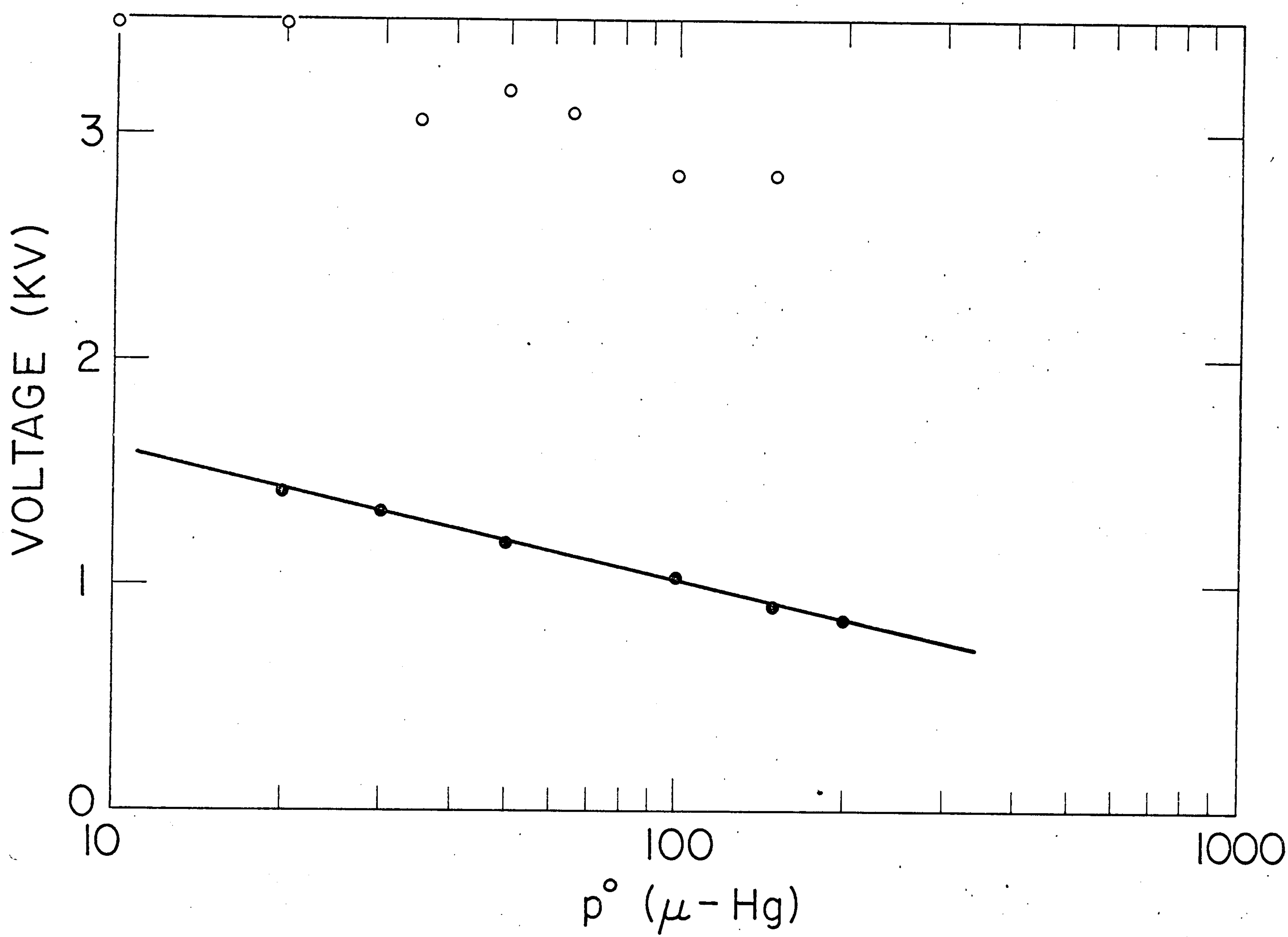

VOLTAGE (KV)
0
1
2
3
10
100
1000
p° (μ-Hg)

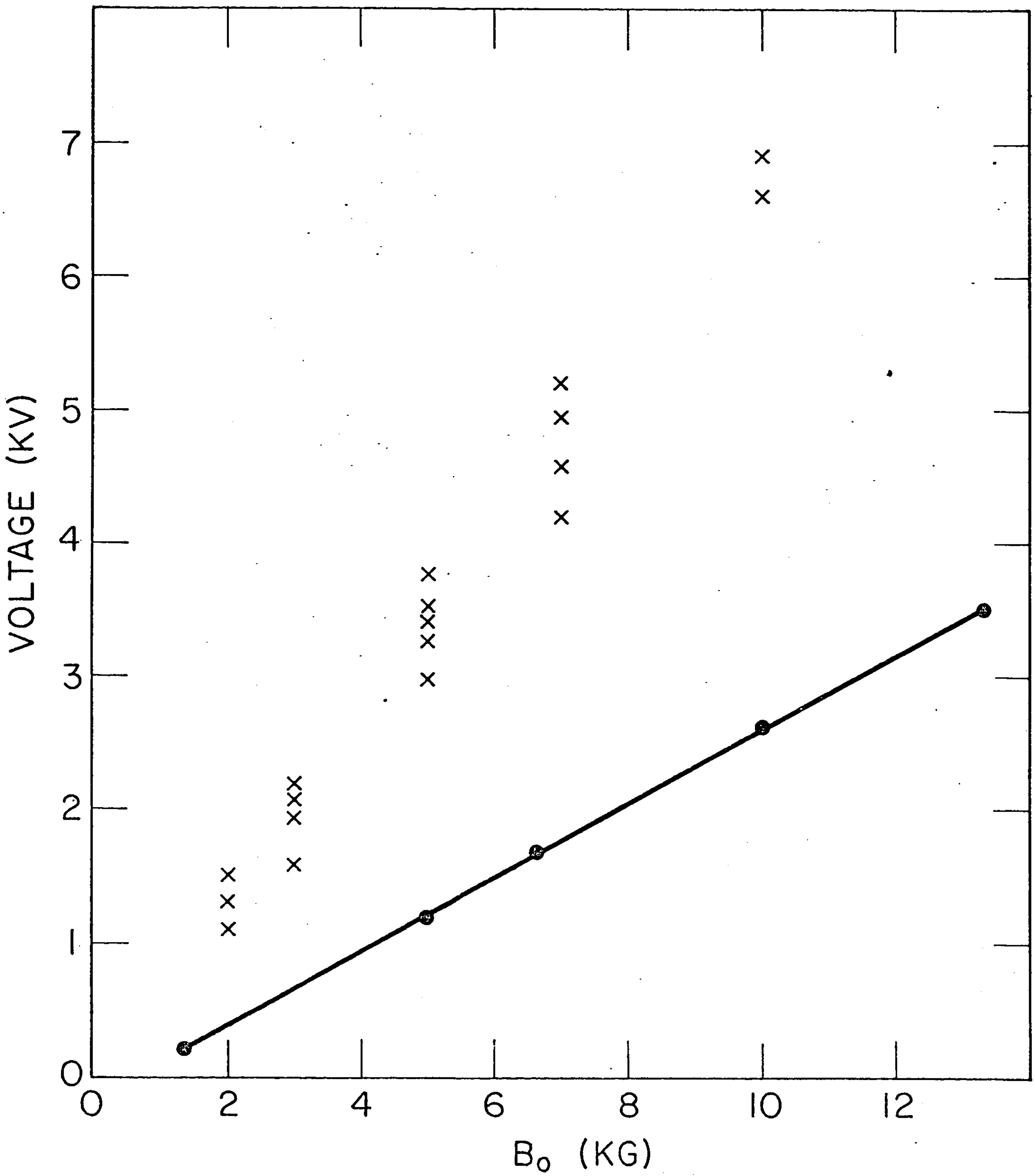

VOLTAGE (KV)
0
1
2
3
4
5
6
7
0
2
4
6
8
10
12
B_o (KG)

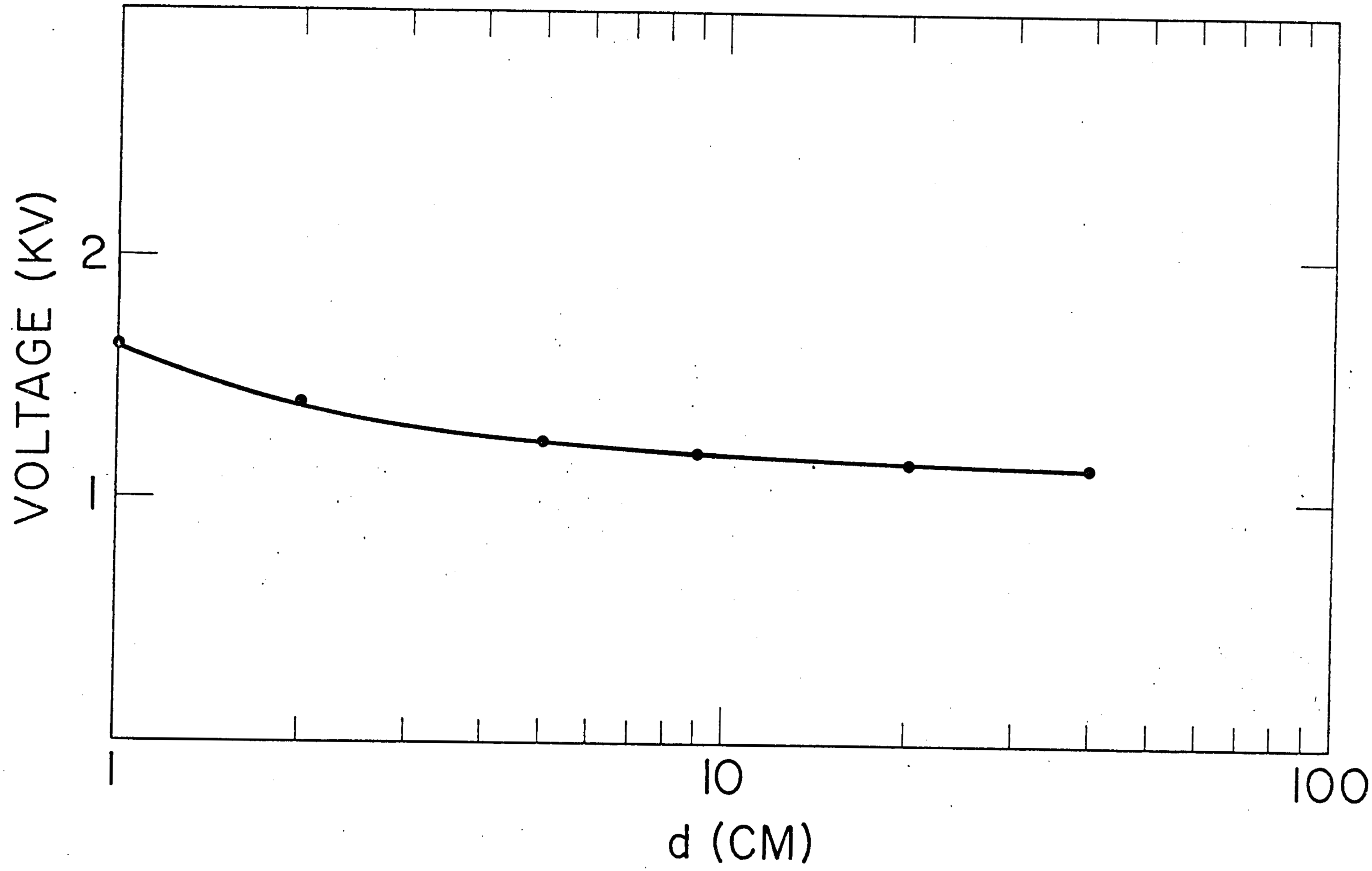
VOLTAGE (KV)
2
1
1
10
100
d (CM)